

Signatures of supersymmetry with non-universal Higgs mass at the Large Hadron Collider

Subhaditya Bhattacharya^{†1}, Sanjoy Biswas^{‡2}, Biswarup Mukhopadhyaya^{‡3}
and Mihoko M. Nojiri^{*4}

[†]*Department of Physics and Astronomy*

University of California, Riverside, California 92521, USA

[‡]*Regional Centre for Accelerator-based Particle Physics*

Harish-Chandra Research Institute

Chhatnag Road, Jhansi, Allahabad - 211 019, India

^{*}*Institute for the Physics and Mathematics of the Universe*

University of Tokyo, Chiba 277-8583, Japan

Theory Group, KEK, 1-1 Oho, Tsukuba, Ibaraki 305-0801, Japan

The Graduate University for Advanced Studies (SOKENDAI)

1-1 Oho, Tsukuba, Ibaraki 305-0801, Japan

Abstract

We discuss large non-universality in the Higgs sector at high scale in supersymmetric theories, in the context of the Large Hadron Collider (LHC). In particular, we note that if $m_{H_u}^2 - m_{H_d}^2$ is large and negative ($\simeq 10^6 \text{ GeV}^2$) at high scale, the lighter slepton mass eigenstates at the electroweak scale are mostly left chiral, in contrast to a minimal supergravity (mSUGRA) scenario. We use this feature to distinguish between non-universal Higgs masses (NUHM) and mSUGRA by two methods. First, we study final states with same-sign ditaus. We find that an asymmetry parameter reflecting the polarization of the taus provides a notable distinction. In addition, we study a charge asymmetry in the jet-lepton invariant mass distribution, arising from decay chains of left-chiral squarks leading to leptons of the first two families, which sets apart an NUHM scenario of the above kind.

¹subhab@ucr.edu

²sbiswas@hri.res.in

³biswarup@hri.res.in

⁴nojiri@post.kek.jp

1 Introduction

With the Large Hadron Collider (LHC) already running, one feels closer than ever to glimpses of physics beyond the standard model (SM). Supersymmetry (SUSY) [1, 2] has always remained an attractive hunting ground in this context. The LHC has brought added impetus to not only the search for SUSY, but also the more ambitious proposal to identify the over-seeing high-scale physics that can lead to typical low-energy spectra. Such high-scale physics is often envisioned as the ‘organizing principle’ behind the plethora of low-scale parameters in the minimal supersymmetric standard model (MSSM) [3, 4] to be seen at low energy. A frequently adopted approach in this direction is to embed MSSM in a minimal supergravity (mSUGRA) scenario [5], where all the low-scale parameters can be generated from:

$$m_{1/2}, m_0, A_0, \tan \beta \text{ and } \text{sgn}(\mu)$$

where $m_{1/2}, m_0, A_0$ are the universal gaugino mass, scalar mass and trilinear scalar coupling parameters respectively at the high-scale, $\tan \beta = \langle H_u \rangle / \langle H_d \rangle$ is the ratio of the two Higgs vacuum expectation values and μ is the SUSY-conserving Higgsino mass parameter in the MSSM superpotential.

However, the mSUGRA model can be branded over-simplistic, as the assumption of universality doesn’t follow from any known symmetry principle. For example, gaugino mass non-universality can occur in supersymmetric Grand Unified Theories (SUSY-GUT) [6] with non-trivial gauge kinetic functions [7, 8]. Non-universality in the scalar sector can also be motivated from the $SO(10)$ D -terms [9], apart from the phenomenological requirement to keep CP-violation and flavour changing neutral currents (FCNC) under control [10]. Also, in mSUGRA, one assumes that the Higgs mass parameters have their origin in the same m_0 which generate squark and slepton masses, which is completely *ad hoc*. For example, in SUSY-GUT theories based on the $SO(10)$ group, sfermions and Higgs fields belong to different representations and can therefore arise from independent high-scale mass parameters. In view of this, one can, within the SUGRA scenario itself, expect the Higgs mass parameters to arise from high scale value(s) different from m_0 . Thus models with non-universal Higgs mass (NUHM) are of considerable interest, and their viability in respect of both collider signals and issues such as the dark matter content of the universe has been recently investigated [11, 12, 13].

One can incorporate the non-universality in the Higgs sector in two different ways. In the first kind, one can have both of the soft Higgs mass parameters originating in a high-scale value m'_0 which is different from m_0 , the universal high-scale mass for squarks and sleptons.

In other words, one can postulate $m_{H_u}^2 = m_{H_d}^2 = m_0'^2 \neq m_0^2$ [12]. On the other hand, it is also possible to have H_u and H_d evolve down from *two different high-scale inputs*. In the later case, the high-scale SUSY parameters are given by:

$$m_{1/2}, m_0, m_{H_u}^2, m_{H_d}^2, A_0, \tan \beta \text{ and } \text{sgn}(\mu)$$

The split between the two Higgs squared masses at high scale introduces additional features in the running of various mass parameters down to the electroweak scale. In its most drastic manifestation, such a situation can give rise to the sneutrino ($\tilde{\nu}$) as the lightest superpartner of standard model particles. Since a sneutrino dark matter candidate is disfavoured from available results on direct search, one then has to postulate the sneutrino(s) to be the next-to-lightest supersymmetric particle(s) (NLSP), and, for example, gravitino as the lightest supersymmetric particle (LSP). With this achieved, most of the allowed region of the NUHM parameter space leads to the right amount of relic density [14].

In this work, we propose using the LHC data to distinguish those cases where the superparticle spectrum in NUHM is most strikingly different from the usual mSUGRA scenario. As we shall see in the next section, this happens for a large negative high-scale value of $m_{H_u}^2 - m_{H_d}^2$. It not only leads to a large splitting between the left and right chiral sleptons, but also leads to the lighter slepton mass eigenstate of any flavour being dominated by the left chiral component.

This feature, marking a drastic departure from the expectations in mSUGRA, can be reflected in the signals of staus through the polarization of the taus that are produced either in their decay or in association with them [15, 16, 17]. In addition, the above hierarchy between left-and right-chiral sleptons can be probed by studying the spin correlation of jets and leptons produced in cascade decays of squarks. This correlation, as we shall see, affects the angular distribution of the lepton in $\chi_2^0 \rightarrow l^\pm \tilde{l}^\mp$, manifested through certain measurable kinematical variables [18, 19, 20].

To explain further, the large splitting between the left-and right-chiral sleptons sometimes yields a hierarchy where the right-chiral ones become much heavier than not only the left-chiral ones but also the low-lying chargino/ second lightest neutralinos over a large region of the NUHM parameter space. Thus they are hardly produced in collider experiments. At the same time, the (dominantly) left-chiral stau and the corresponding sneutrino being considerably lighter — even lighter than the lightest neutralino — the taus produced in their association are dominantly left-handed. This is due to the fact that the gauge couplings involved in the decay are chirality conserving, so long as one has large gaugino components in the lighter neutralinos and charginos.

The consequences that we focus on are two-fold. First, one notices the practically ubiquitous τ in SUSY signals. Secondly, the signals often bear the stamp of left-polarized τ^- 's, in the products of their one-prong decay. With this in view, we analyze the polarization of the taus produced in the SUSY cascades in the same-sign di-tau ($SSD\tau$) final states associated with hard jets and missing transverse energy (E_T). We show how this leads to noticeable differences between the NUHM and mSUGRA spectra in the LHC environment.

Furthermore, we study the polarization dependence of the angular distribution of the lepton produced in χ_2^0 decay, which shows up in the charge asymmetry in the m_{ql} distribution. Though the effect tends to wash out due to the presence of antisquark decay, nevertheless it can be observed at the LHC as more squarks are produced than antisquarks.

This paper is organized as follows. We discuss various aspects of the model under consideration in the following section and identify the region of the $m_0 - m_{1/2}$ parameter space where the lighter stau is dominantly left-chiral. As we shall see below, this is achieved for large negative values of S . We choose a few benchmark points for our collider simulation. Tau-polarization and its implications are discussed in section 3, while the analysis revealing the chirality information on sleptons of the first two families is outlined in section 4. The numerical results for each of the two analyses mentioned above, based on a simulation for the 14 TeV run of the LHC, is presented in section 5. We summarise and conclude in section 6.

2 Features of the NUHM scenario and our choice of benchmark points

2.1 Salient features of the scenario

We consider the general case of NUHM, having a two-parameter extension of the mSUGRA scenario, in which the soft SUSY breaking masses $m_{H_u}^2$ and $m_{H_d}^2$ are inputs at high scale. The most important thing to remember here is that the renormalisation group evolution (RGE) of soft scalar masses is in general modified by the presence of a non-zero boundary value of the quantity S , defined as [3]

$$S = m_{H_u}^2 - m_{H_d}^2 + Tr [\mathbf{m}_Q^2 - \mathbf{m}_L^2 - 2\mathbf{m}_U^2 + \mathbf{m}_D^2 + \mathbf{m}_E^2] \quad (1)$$

We assume universality in the sfermion masses, so that $S = m_{H_u}^2 - m_{H_d}^2$ is high scale

boundary condition. The running of soft scalar masses of the third family squarks and sleptons are given at the one-loop level by [3]

$$\frac{dm_{Q_3}^2}{dt} = \frac{2}{16\pi^2} \left(-\frac{1}{15}g_1^2M_1^2 - 3g_2^2M_2^2 - \frac{16}{3}g_3^2M_3^2 + \frac{1}{10}g_1^2S + y_t^2X_t + y_b^2X_b \right) \quad (2)$$

$$\frac{dm_{\tilde{t}_R}^2}{dt} = \frac{2}{16\pi^2} \left(-\frac{16}{15}g_1^2M_1^2 - \frac{16}{3}g_3^2M_3^2 - \frac{2}{5}g_1^2S + 2y_t^2X_t \right), \quad (4)$$

$$\frac{dm_{\tilde{b}_R}^2}{dt} = \frac{2}{16\pi^2} \left(-\frac{4}{15}g_1^2M_1^2 - \frac{16}{3}g_3^2M_3^2 + \frac{1}{5}g_1^2S + 2y_b^2X_b \right), \quad (5)$$

$$\frac{dm_{L_3}^2}{dt} = \frac{2}{16\pi^2} \left(-\frac{3}{5}g_1^2M_1^2 - 3g_2^2M_2^2 - \frac{3}{10}g_1^2S + y_\tau^2X_\tau \right), \quad (6)$$

$$\frac{dm_{\tilde{\tau}_R}^2}{dt} = \frac{2}{16\pi^2} \left(-\frac{12}{5}g_1^2M_1^2 + \frac{3}{5}g_1^2S + 2y_\tau^2X_\tau \right). \quad (7)$$

where the notations for squark, slepton and gaugino masses have their usual meaning, and $t = \log(Q)$, $y_{t,b,\tau}$ are the t , b and τ Yukawa couplings, and

$$X_t = m_{Q_3}^2 + m_{\tilde{t}_R}^2 + m_{H_u}^2 + A_t^2, \quad (8)$$

$$X_b = m_{Q_3}^2 + m_{\tilde{b}_R}^2 + m_{H_d}^2 + A_b^2, \quad (9)$$

$$X_\tau = m_{L_3}^2 + m_{\tilde{\tau}_R}^2 + m_{H_d}^2 + A_\tau^2 \quad (10)$$

Mass parameters of the first two family scalars run in a similar manner, excepting that the Yukawa contributions are vanishingly small. The main difference in the SUSY particle spectrum with respect to an mSUGRA scenario is the non-vanishing boundary value of S . If this boundary value is large in magnitude, the effect on the spectrum at low scale is naturally a rather pronounced departure from mSUGRA. Since the contribution of the term containing S comes with different factors in the running of left-handed squarks (sleptons) and right-handed squarks (sleptons), due to different $U(1)$ hypercharge assignments, one can have large splitting in the left-right sector within each generation when $|S|$ is substantially large.

One can see from equation (6) and (7) that the effect of non-universal Higgs mass is rather pronounced in the slepton sector, the primary reason being that the running masses are not controlled by the strong sector. The most important difference it makes to the spectrum is that, for large negative values of S ($\mathcal{O}(\text{TeV})^2$) [11, 12], the left-chiral sleptons tend to become considerably lighter than their right-chiral counterparts. This is in striking contrast to both mSUGRA and gauge mediated SUSY breaking (GMSB). An immediate temptation that the phenomenologist faces, therefore, is to extract some signature of this

‘chirality swap’ in the lightest sleptons at the LHC, which may put a distinctive stamp of NUHM on them. This, of course, has to be done with the help of leptons that are produced either in association with the low-lying sleptons or in their decays. Since the helicity of leptons of the first two families is difficult to measure in the collider environment, we feel that it is our best bet to latch on to the copious number of taus arising from SUSY cascades, and concentrate on those features of their decay products that tell us about their helicities.

As has been noted already, the above effect is seen for large negative S . Such values of S therefore become the benchmarks for testing the special features of NUHM, and it is likely that in such condition only its footprints are noticeable at the LHC. Thus we examine next the kinds of spectra ensuing from large negative S , and look for their observable signature.

A large negative S at high scale affects the running of the third family SU(2) doublet slepton (both the stau and the tau-sneutrino) masses in the same way as is done by their Yukawa couplings, thus bringing them down substantially at low energy. As a consequence, one can have both of them of the same order as, or lighter than, the lightest neutralino (χ_1^0). In the latter situation, the left-chiral tau-sneutrino is lighter than the corresponding stau due to the SU(2) breaking D-terms (for $\tan \beta > 1$) :

$$m_{\tilde{\tau}_L}^2 = m_L^2 - \cos(2\beta)m_Z^2\left(\frac{1}{2} - \sin^2 \theta_W\right) \quad (11)$$

$$m_{\tilde{\nu}_\tau}^2 = m_L^2 + \cos(2\beta)m_Z^2\frac{1}{2} \quad (12)$$

In such cases, the tau-sneutrino has to be the NLSP, due to its unsuitability as a dark matter candidate as laid down by direct search results. A gravitino, for example, can be envisioned as the LSP and dark matter candidate in such cases. The lighter stau mass eigenstate can in principle also become the NLSP through mixing of the left and right chiral fields. However, this happens only in very restricted regions of the parameter space, as large mixing requires $\tan \beta$ to be on the higher side, a feature that is highly restricted in NUHM by the requirements of absence of tachyonic states as well as of electroweak symmetry breaking.

The role of S in the running of $m_{H_u}^2$ and $m_{H_d}^2$ is described by

$$\frac{dm_{H_u}^2}{dt} = \frac{2}{16\pi^2} \left(-\frac{3}{5}g_1^2M_1^2 - 3g_2^2M_2^2 + \frac{3}{10}g_1^2S + 3f_t^2X_t \right), \quad (13)$$

$$\frac{dm_{H_d}^2}{dt} = \frac{2}{16\pi^2} \left(-\frac{3}{5}g_1^2M_1^2 - 3g_2^2M_2^2 - \frac{3}{10}g_1^2S + 3f_b^2X_b + f_\tau^2X_\tau \right), \quad (14)$$

One can see above that a negative S tends to partially cancel the effects of top quark Yukawa coupling in the running of $m_{H_u}^2$ and make it positive at low energy. $m_{H_d}^2$, on the

other hand, is routinely rendered positive at low scale due to the gauge interactions, and the effects of the term proportional to S often fails to make it negative as one comes down to the electroweak scale. Consequently, radiative electroweak symmetry breaking at the right energy requires a negative value of $m_{H_u}^2$ at high scale. Of course, one is led to have a sufficiently large magnitude of μ to ensure that $m_{H_u}^2 + \mu^2$ remains positive at high energy.

2.2 The choice of benchmark points

As has been already explained, our purpose is to suggest some observations at the LHC, which will bring out the distinctive characteristics of the NUHM spectrum. Such distinction is most pronounced when the chiralities of the low-lying sleptons are reversed with respect to the corresponding cases in mSUGRA. This, we have found, is best achieved (and one is indeed optimistic about clear distinction) when S is large and negative ($\sim 10^6 \text{ GeV}^2$). For smaller magnitudes of S ($\leq 10^5 \text{ GeV}^2$), the $\tilde{\tau}_L$ component of $\tilde{\tau}_1$ decreases, and the collider signature of this scenario is relatively less distinct. With this in view, the region in the parameter space with more than 90% of $\tilde{\tau}_L$ in $\tilde{\tau}_1$ has been shown in Figure 1. This region offers the best hope for recognising NUHM if SUSY is detected at the LHC. We have accordingly chosen some benchmark points for the study reported in the subsequent sections. Out of the regions answering to our chosen criterion, we have selected points with three possible mass hierarchies:

$$\begin{aligned} m_{\tilde{\nu}_{\tau_L}} &< m_{\chi_1^0} < m_{\tilde{\tau}_1} \\ m_{\tilde{\nu}_{\tau_L}} &< m_{\tilde{\tau}_1} < m_{\chi_1^0} \\ m_{\chi_1^0} &< m_{\tilde{\nu}_{\tau_L}} < m_{\tilde{\tau}_1} \end{aligned}$$

Our benchmark points (BP) NUHM-1 - NUHM-3 (shown in Table 1) are taken from three regions of the parameter space, corresponding to each of the above hierarchies. The code SuSpect (version 2.41)[21] has been used for this purpose. Two-loop renormalisation group equations have been used for running the mass parameters down to low energy, with the default option (namely, $\sqrt{\tilde{t}_1 \tilde{t}_2}$) for the electroweak symmetry breaking scale. The spectra are consistent with low energy constraints [22, 23] such as those coming from $b \rightarrow s\gamma$ and the muon anomalous magnetic moment, and also with those from LEP-2 limits, such as $m_{\chi_1^\pm} > 103.5 \text{ GeV}$, $m_{\tilde{l}^\pm} > 98.8 \text{ GeV}$ and $m_h > 111 \text{ GeV}$. Electroweak symmetry breaking in a consistent fashion has been taken as a necessary condition in the allowed parameter space. For the case with χ_1^0 LSP, the requirement of relic density consistent with the recent data has also been taken into account in choosing the benchmark point(s) [24].

Benchmark points	NUHM-1	NUHM-2	NUHM-3
Input parameters	$m_0 = 300$ $m_{1/2} = 300$ $\tan \beta = 10$	$m_0 = 80$ $m_{1/2} = 460$ $\tan \beta = 10$	$m_0 = 300$ $m_{1/2} = 280$ $\tan \beta = 7$
$m_{\tilde{e}_L}, m_{\tilde{\mu}_L}$	170	154	154
$m_{\tilde{e}_R}, m_{\tilde{\mu}_R}$	552	437	551
$m_{\tilde{\nu}_{e_L}}, m_{\tilde{\nu}_{\mu_L}}$	151	132	133
$m_{\tilde{\nu}_{\tau_L}}$	119	106	116
$m_{\tilde{\tau}_1}$	139	124	137
$m_{\tilde{\tau}_2}$	537	424	543
$m_{\chi_1^0}$	120	187	112
$m_{\chi_2^0}$	234	361	216
$m_{\chi_3^0}$	939	982	950
$m_{\chi_4^0}$	944	987	954
$m_{\chi_1^\pm}$	234	361	217
$m_{\chi_2^\pm}$	944	987	955
$m_{\tilde{g}}$	734	1066	691
$m_{\tilde{t}_1}$	645	826	618
$m_{\tilde{t}_2}$	814	1018	791
$m_{\tilde{d}_L}$	741	986	706
$m_{\tilde{d}_R}$	742	962	710
$m_{\tilde{u}_L}$	737	984	701
$m_{\tilde{u}_R}$	591	879	549
m_{h^0}	111	114	112

Table 1: *Proposed benchmark points for the study of the NUHM scenario with $m_{H_u}^2 = -1.10 \times 10^6 \text{ GeV}^2$ and $m_{H_d}^2 = 2.78 \times 10^6 \text{ GeV}^2$. All the mass parameters are given in units of GeV. The value of A_0 is taken to be zero and sign of μ to be positive for all of the benchmark points.*

Benchmark points	mSUGRA-1	mSUGRA-2	mSUGRA-3
Input parameters	$m_0 = 80$ $m_{1/2} = 250$ $\tan \beta = 40$	$m_0 = 350$ $m_{1/2} = 300$ $\tan \beta = 40$	$m_0 = 300$ $m_{1/2} = 350$ $\tan \beta = 10$
$m_{\tilde{e}_L}, m_{\tilde{\mu}_L}$	389	362	284
$m_{\tilde{e}_R}, m_{\tilde{\mu}_R}$	363	322	202
$m_{\tilde{\nu}_{e_L}}, m_{\tilde{\nu}_{\mu_L}}$	381	354	271
$m_{\tilde{\nu}_{\tau_L}}$	353	329	269
$m_{\tilde{\tau}_1}$	283	238	197
$m_{\tilde{\tau}_2}$	377	358	285
$m_{\chi_1^0}$	99	120	140
$m_{\chi_2^0}$	183	224	261
$m_{\chi_3^0}$	333	392	455
$m_{\chi_4^0}$	352	409	473
$m_{\chi_1^\pm}$	182	224	262
$m_{\chi_2^\pm}$	353	410	473
$m_{\tilde{g}}$	623	726	831
$m_{\tilde{t}_1}$	464	525	573
$m_{\tilde{t}_2}$	615	683	764
$m_{\tilde{d}_L}$	654	720	776
$m_{\tilde{d}_R}$	636	697	745
$m_{\tilde{u}_L}$	649	716	771
$m_{\tilde{u}_R}$	636	698	747
m_{h^0}	111	112	111

Table 2: *mSUGRA* benchmark points obtained based on similar cross-section in the same-sign ditau channel (*mSUGRA-1* and *mSUGRA-2*) and in the opposite-sign same-flavor dilepton channel (*mSUGRA-3*). All the mass parameters are given in units of *GeV*. The value of A_0 is taken to be zero and sign of μ to be positive for all of the benchmark points.

We have obtained the mSUGRA BP's for comparison with the NUHM points using the criterion based on similar event rates (within $\pm 30\%$ tolerance) in two different channels. For the case where the distinction between these two scenarios is done using tau-polarisation, we have compared the event rates in the same-sign ditau ($SSD\tau$) channel for choosing our mSUGRA points. For the analysis based upon lepton-charge asymmetry, the event rates in the opposite-sign same-flavor dilepton ($OSSF\ell\ell$) channel have been compared as a benchmarking criterion. All the three NUHM BP's have been used for the first case and for the second case, only NUHM-1 and NUHM-3 have been considered, as the hierarchies mentioned above are not relevant for analysis based on lepton-charge asymmetry. Thus, we have obtained mSUGRA-1 which corresponds to both NUHM-1 and NUHM-3 following the criterion mentioned above in the $SSD\tau$ channel and mSUGRA-3 corresponds to NUHM-3 in the $OSSF\ell\ell$ channel. The benchmark point mSUGRA-2 corresponds to NUHM-2 having similar rates in the $SSD\tau$ channel. Two of the chosen mSUGRA points (mSUGRA-1 and mSUGRA-2) are approximately compatible with the observed relic density.

The values of various SUSY parameters in the chosen points are listed in Table 1. One has to further assume in the case of $\tilde{\nu}_\tau$ -NLSP and gravitino (\tilde{G}) LSP that the decay $\tilde{\nu}_\tau \rightarrow \nu_\tau \tilde{G}$ does not have a lifetime exceeding the age of the universe. The gravitino mass has to have accordingly allowed values, as dictated by the hidden sector of the overseeing theory [25].

3 Tau polarisation

The signal of left-polarised tau is expected to be a very good discriminator between scenarios with NUHM and its universal counter part. Tau lepton plays a crucial role in the search for new physics. In particular, information on the chirality of a tau can be extracted following some standard procedures. The fact that the tau decays within the detector, in contrast to the electron or the muon, enables us to know about its chirality from the kinematic distribution of the decay products. In the massless limit where the tau is boosted in the laboratory frame, tau decay products are nearly collinear with the parent tau. In this limit, hadronic tau decays produce narrow jets of low multiplicity, to be identified as tau-jets. From the angle of polarisation studies, it is most cost-effective to work with the one-prong hadronic decay modes of the tau, which comprise 80% of its hadronic decay width and about 50% of its total decay width. The main channels here are:

$$\tau^- \rightarrow \pi^- \nu_\tau$$

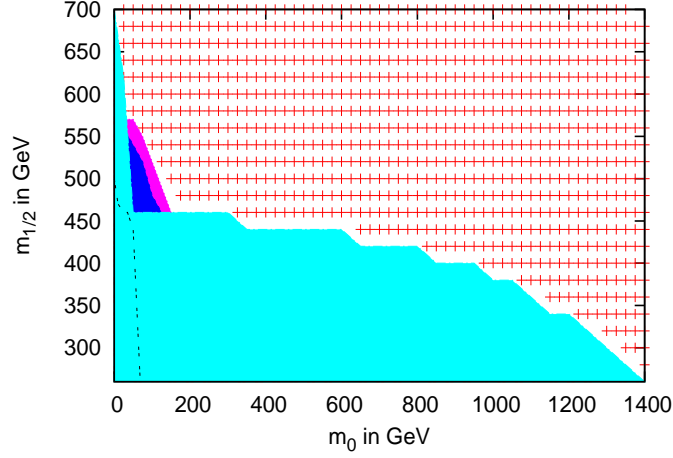


Figure 1: *The allowed region for NUHM in the $m_0 - m_{1/2}$ plane for $\tan\beta = 10$, $m_{H_u}^2 = -1.0 \times 10^6 \text{ GeV}^2$, $m_{H_d}^2 = 2.0 \times 10^6 \text{ GeV}^2$ and $A_0 = 0$. The light blue region is disallowed due to tachyonic stau and/or non-compliance of electroweak symmetry breaking conditions. The region on the left of the dashed line is also disallowed by constraints from $b \rightarrow s\gamma$. In the region marked by +, one has $m_{\chi_1^0} < m_{\tilde{\nu}_{\tau L}} < m_{\tilde{\tau}_1}$, whereas the pink region corresponds to $m_{\tilde{\nu}_{\tau L}} < m_{\chi_1^0} < m_{\tilde{\tau}_1}$. The dark blue region has the hierarchy $m_{\tilde{\nu}_{\tau L}} < m_{\tilde{\tau}_1} < m_{\chi_1^0}$. The lighter stau has 90% or more of $\tilde{\tau}_L$ over the entire allowed region.*

$$\begin{aligned}\tau^- &\rightarrow (\rho^- \nu_\tau) \rightarrow \pi^- \pi^0 \nu_\tau \\ \tau^- &\rightarrow (a_1^- \nu_\tau) \rightarrow \pi^- \pi^0 \pi^0 \nu_\tau\end{aligned}$$

where we shall often denote both the ρ^- and the a_1^- by v .

The first step in the extraction of polarisation information is to express some differential decay distributions of the τ^- in the laboratory frame. Let the polarisation information be denoted by P_τ , where $P_\tau = \pm 1$ correspond to taus with positive and negative helicity. Next, it is worthwhile to examine the laboratory frame variable z , defined as $z = E_{\pi, v}/E_\tau$, the fraction of the tau energy carried by the product meson. This variable can be related to θ , the angle between the direction of motion of the outgoing π^- or v^- and the axis of polarisation of the tau, which is taken to be along the direction of the tau momentum in the laboratory frame. In the limit $E_\tau \gg m_\tau$,

$$\cos \theta = \frac{2z - 1 - c^2}{1 - c^2} \quad (15)$$

where $c = m_v/m_\tau$. The expression for the case where the tau decays to the pion and a ν_τ is obtained by setting $m_v = 0$ above.

The decay distributions in z for a τ^- in the laboratory frame are given by [26]

$$\frac{1}{\Gamma_\pi} \frac{d\Gamma_\pi}{dz} = [1 + P_\tau(2z - 1)] \quad (16)$$

$$\begin{aligned} \frac{1}{\Gamma_v} \frac{d\Gamma_{v_L}}{dz} = & \frac{m_\tau^2 m_v^2}{(m_\tau^2 - m_v^2)(m_\tau^2 + 2m_v^2)} \left[\frac{m_\tau^2}{m_v^2} \sin^2 \omega + 1 + \cos^2 \omega + P_\tau \cos \theta \right. \\ & \left. \left(\frac{m_\tau^2}{m_v^2} \sin^2 \omega - \frac{m_\tau}{m_v} \sin 2\omega \tan \theta - 1 - \cos^2 \omega \right) \right], \end{aligned} \quad (17)$$

$$\begin{aligned} \frac{1}{\Gamma_v} \frac{d\Gamma_{v_T}}{dz} = & \frac{m_\tau^2 m_v^2}{(m_\tau^2 - m_v^2)(m_\tau^2 + 2m_v^2)} \left[\frac{m_\tau^2}{m_v^2} \cos^2 \omega + \sin^2 \omega + P_\tau \cos \theta \right. \\ & \left. \left(\frac{m_\tau^2}{m_v^2} \cos^2 \omega + \frac{m_\tau}{m_v} \sin 2\omega \tan \theta - \sin^2 \omega \right) \right] \end{aligned} \quad (18)$$

where

$$\cos \omega = \frac{(m_\tau^2 - m_v^2) + (m_\tau^2 + m_v^2) \cos \theta}{(m_\tau^2 + m_v^2) + (m_\tau^2 - m_v^2) \cos \theta} \quad (19)$$

In the experiment, one looks for hard jets from the tau, which corresponds to large values of z . A close inspection of Equations (16),(17),(18) shows that the energy distribution of the decay products from the decay of τ_L^- ($P_\tau = -1$) are in significant contrast to that from τ_R^- ($P_\tau = +1$). When $P_\tau = +1$, the hard τ -jet consist largely of either a single pion or longitudinally polarised vector mesons (v_L). For $P_\tau = -1$, on the contrary, the hard τ -jet mostly comprises transversely polarised vector mesons only (v_T). This conclusion becomes almost self-evident in, for example, the extreme case of collinearity, with $\cos \omega = 1$ and $\sin \omega = 0$.

It should, however, be remembered that the quantity z is not amenable to actual measurement in the detector, and therefore the distinctions pointed out above are still somewhat theoretical in nature. It is therefore necessary to translate the distinction in terms of measurable quantities. The energy distribution among the pions arising from the decay of the ρ^- and a_1^- offer such a variable. It is the variable $R = E_\pi/E_\rho$, the fraction of the energy of v carried by the charged pion. For the case where the ρ^- is produced in τ^- decay, the distribution in R in the laboratory frame is given by [26]

$$\frac{d\Gamma(\rho_T \rightarrow 2\pi)}{dR} \sim 2R(1 - R) - \frac{2m_\pi^2}{m_\rho^2} \quad (20)$$

$$\frac{d\Gamma(\rho_L \rightarrow 2\pi)}{dR} \sim (2R - 1)^2 \quad (21)$$

The distribution for a_1^- is more complicated but has similar qualitative features. The reader is referred to [27] for the detailed expressions. The broad indication is that transversely polarised vector mesons favour even sharing of its momentum among the decay pions whereas longitudinally polarised ones favour uneven sharing of momentum among its decay products. Since the polarisation of the parent tau governs the level of polarisation of either type in the vector mesons v , the distribution in the variable R therefore is a reflection of the helicity of the tau whose signal one is concerned with.

Obviously, one always has $R = 1$ when the tau decays as $\tau^- \rightarrow \pi^- \nu_\tau$. What one must utilise, therefore, is the difference in R -distributions between the cases with v_T and v_L . When the decaying tau has $p_\tau = +1$, one should mostly have v_L in the hard jets, in addition to the inconsequential single pions, giving its characteristic distribution on R . A contrast can be seen in the decay of a tau with $p_\tau = -1$, where the hard tau-jets can be expected to be largely v_T , with a different distribution in R .

Hence, one can use the charged-pion spectra arising from the two-stage decays

$$\begin{aligned}\tau^- &\rightarrow (\rho^- \nu_\tau) \rightarrow \pi^- \pi^0 \nu_\tau \\ \tau^- &\rightarrow (a_1^- \nu_\tau) \rightarrow \pi^- \pi^0 \pi^0 \nu_\tau\end{aligned}$$

to probe the polarisation of the parent tau. We utilise this possibility to identify the NUHM spectrum in cases the low-lying stau is of left chirality, which attaches similar chirality (same as helicity at high energy) to the taus either arising from stau-decay or produced in association with it. With this in view, we have selected tau-jets in our simulation with $p_T > 40 \text{ GeV}$ and $|\eta| < 2.5$, assuming a tau jet identification efficiency of 50%, with a fake tau jet rejection factor of 100 [16].

4 Lepton charge asymmetry

Another discriminator which is sensitive to the mass hierarchy between the right-and left-chiral sleptons is the charge asymmetry in the jet-lepton invariant mass distribution [18, 19, 20]. In the NUHM scenario (with large negative S), the lighter slepton mass eigenstate is dominated by the left-chiral component ($\tilde{l}_1 \sim \tilde{l}_L$). Hence, for $m_{\tilde{l}_1} < m_{\chi_2^0}$ (a criterion mostly satisfied by the ‘extreme’ NUHM scenario considered by us), the leptons produced in the decay of χ_2^0 will be mostly left-handed. In the usual mSUGRA scenario, on the other hand, one expects the leptons to be mostly right-handed as the lighter slepton mass eigenstate is dominantly right-chiral ($\tilde{l}_1 \sim \tilde{l}_R$) and the decay proceeds via the Bino component of χ_2^0 .

This feature can be exploited to unmask NUHM by studying the charge asymmetry in the lepton-jet invariant mass (m_{jl_1}) distribution produced in the squark decay chains, where l_1 stands for the lepton reproduced in χ_2^0 decay. We shall consider sleptons of the first two generations only, for which left-right mixing is negligible, and the coupling of the leptons to the Higgsino components of a neutralino is also very small.

In this section we describe the spin correlation in the following decay chain

$$\tilde{q}_L \rightarrow q\chi_2^0 \rightarrow ql_1^\pm \tilde{l}^\mp \rightarrow ql_1^\pm l_2^\mp \chi_1^0 \quad (22)$$

where l_2 denotes the lepton produced in the subsequent step of the cascade. Due to the chiral structure of the squark-quark-neutralino coupling, the quark produced in the squark decay will be left-handed in the massless limit. The χ_2^0 produced in \tilde{q}_L decay is also polarized having the same helicity as that of the quark as they are produced from the decay of a scalar.

In the rest frame of the squark produced in the initial hard scattering, a negatively charged lepton produced in the subsequent decay of the χ_2^0 will appear back-to-back or in the same direction as that of the quark depending on whether the slepton is left-chiral or right-chiral.¹ Exactly the opposite directional preferences hold for a (positively charged) antilepton vis-a-vis the quark produced in the chain. Therefore, we expect an asymmetry between the distributions $m_{jl_1^-}$ and $m_{jl_1^+}$. This can be utilised to define the following asymmetry parameter:

$$A_i = \frac{N_i(m_{jl_1^+}) - N_i(m_{jl_1^-})}{N_i(m_{jl_1^+}) + N_i(m_{jl_1^-})} \quad (23)$$

where i stands for the i th bin. A measurement A_i should thus yield information on the chirality of the low-lying slepton produced in the chain.

However, there are some experimental difficulties involved in the measurement of such an asymmetry—

1. In the decay of a \tilde{q}_L^* , the asymmetry in the lepton-jet invariant mass distribution has a sign opposite to that of the corresponding \tilde{q}_L . This is because the left antisquark decays via gaugino coupling into a right-handed antiquark. Since jets initiated by a quark or an anti-quark are indistinguishable, it is impossible to disentangle the squark and antisquark production channels. However, the LHC is a pp machine where more

¹The other inputs that go into this argument are (a) The χ_2^0 produced in squark decay is sufficiently boosted, and (b) the χ_2^0 decays largely in the s-wave.

squarks are produced than anti-squarks, a significant ‘net’ charge asymmetry in the m_{jl_1} distribution can finally survive. All one needs in order to measure this charge asymmetry is a substantial excess in the production of $\tilde{q}^{(*)}\tilde{g}$ and $\tilde{q}^{(*)}\tilde{q}^{(*)}$ over pairs containing squarks and antisquarks, and also gluino pairs.

2. In an experiment, it is not always possible to distinguish between the lepton (l_1) out of a χ_2^0 and the lepton (l_2) coming from slepton decay. We have taken the invariant mass distribution using the harder of the two leptons, a role in which l_1 fits in most of the time.

In NUHM, one expects negative charge asymmetries, whereas in the usual mSUGRA scenario they are expected to be positive, especially in the high invariant mass bins. However, in mSUGRA, depending on the mass hierarchy, the leptons produced in χ_2^0 decay can also be dominantly left-handed if $m_{\tilde{l}_1} < m_{\tilde{l}_2} < m_{\chi_2^0}$, as the diagonal component ($(U_N)_{22}$) of the neutralino mixing matrix wins over $(U_N)_{21}$. In that case, one would expect a dip in the asymmetry distribution at a lower value of m_{jl} and a peaking behaviour at the higher end. This is expected because the splitting between $m_{\chi_2^0}$ and \tilde{l}_L is smaller than that between $m_{\chi_2^0}$ and \tilde{l}_R . One can use this feature to separate an mSUGRA-type scenario.

5 Collider simulation and numerical results

We have simulated events for $\sqrt{s} = 14$ TeV, including initial-and final-state radiation, multiple scattering etc. We have used parton distribution functions CTEQL6L1 [28] for our analysis, with the renormalisation and factorisation scales set at the average mass of the final state particles.

5.1 Simulation strategy: ditau final states

To study the polarisation of the tau in SUSY cascade for both NUHM and mSUGRA scenario we have used the code TAUOLA (version 2.9) [29] interfaced with the event generator PYTHIA (version 6.4.16) [30]. The spectrum has been generated using SuSpect (version 2.41) [21]. TAUOLA has been suitably modified to incorporate the probability of producing left-or right-handed tau in the decay of SUSY particles. For cases where the $\tilde{\nu}_\tau$ and/or the $\tilde{\tau}$ is lighter than the lightest neutralino, decay branching fractions of the lightest neutralino have been calculated using SDECAY (version 1.3b) [31] and fed into Pythia. The

finite detector resolutions have been taken into account following the specifications listed, for example, in [32].

The final state that we have considered is a pair of same-sign ditaus ($SSD\tau$), together with at least three hard central jets and large missing E_T . Same-sign ditaus are preferred because they are less beset with SM backgrounds. We consider events where the taus have one-prong hadronic decays.

The following cuts have been imposed on each event–

- $p_T > 40$ GeV, $|\eta| < 2.5$ for each tau jet.
- $p_T > 100, 100, 50$ GeV, $|\eta| < 2.5$ for the three associated jets, in decreasing order of hardness.
- $E_T > 150$ GeV.

It should be reiterated that our main purpose is to obtain the observable difference between the NUHM scenario under consideration and an mSUGRA scenario. Situations in mSUGRA leading to tau-rich final states are most likely to fake NUHM phenomenology. Therefore, we have followed the criteria already mentioned in section 2.2, and isolated the regions where the total rate of $SSD\tau + \geq 3 \text{ jets} + E_T$ is within $\pm 30\%$ of the rate predicted for corresponding NUHM benchmark point.

5.2 Simulation strategy: lepton charge asymmetry

The charge asymmetry in the lepton-jet invariant mass distribution has been studied using the event generator HERWIG (version 6.5) [33] which takes into account the spin correlation in SUSY cascades. Spectra have been generated using ISAJET (version 7.78) [34] and the input parameters have been tuned in such a way that the spectrum generated is similar to that produced by SuSpect. A fast detector simulation has been done using AcerDET (version 1.0) [35] for reconstructing the isolated leptons, jets and E_T , which also takes into account the finite detector resolution of the visible momenta.

The final state under consideration is consists of a pair of isolated leptons of opposite charge and same flavor (OSSF) with more than three jets and missing E_T , i.e., $e^+e^- + \mu^+\mu^- + \geq 3 \text{ jets} + E_T$.

The preselection cuts [36, 37] imposed in this case are the following–

- $p_{T_{l_1}} > 20$ GeV and $p_{T_{l_2}} > 10$ GeV, $|\eta| < 2.5$ for the two leptons.

- $p_T > 100, 50, 50$ GeV, $|\eta| < 2.5$ for the three associated jets, in decreasing order of hardness.
- $M_{eff} > 600$ GeV where, $M_{eff} = E_T + \Sigma|\vec{p}_T|$
where, the summation is taken over all visible particles.
- $E_T > 0.2M_{eff}$

The SUSY backgrounds come mainly from two independent χ_1^\pm decay. One can eliminate this by taking the flavor subtracted combination $e^+e^- + \mu^+\mu^- - e^\pm\mu^\mp$ and this cancels out the background contribution from the charginos up to statistical fluctuations. The Standard Model background, already small after imposing the above cuts, undergo further suppression in this process [37].

The leptons are combined with each of the two hardest jets and, for identifying the desired decay chain, the combination for which the $jl^{+}l^{-}$ invariant mass is smaller has been selected. The m_{jl^\pm} distribution for this subsample, for both the hard and soft lepton have been calculated. Depending on the mass splitting between the neutralino and slepton one of these leptons will be dominated by the 'correct' lepton, i.e., the one adjacent to the quark in the decay chain and will give the desired charge asymmetry in the jet-lepton invariant mass distribution.

5.3 Numerical results

Ditau final states:

We first present the numerical results of our analysis using of the polarisation properties of the tau. In Table 2, we have tabulated the event rates for all the NUHM and the potentially faking mSUGRA points for the $SSD\tau$ -channel. Event rates have been predicted for an integrated luminosity of 100 fb^{-1} . After applying all the cuts to suppress the SM background, one has similar event rates for both the NUHM and corresponding mSUGRA points, which is not surprising because we have identified the mSUGRA points following the criterion of similar event rate.

For the benchmark point NUHM-1, $\tilde{\nu}_{\tau_L}$ is the LSP, and the lighter $\tilde{\tau}_1$ is dominantly left-chiral. Taus are mainly produced in the decay of $\chi_2^0 \rightarrow \tau\tilde{\tau}$ (20.5%), $\chi_1^\pm \rightarrow \tau\tilde{\nu}_{\tau_L}$ (26.5%) and $\tilde{\tau} \rightarrow \tau\chi_1^0$ (100%) and therefore the taus are mostly left-handed. The contributions from χ_3^0 , χ_4^0 , χ_2^\pm and $\tilde{\tau}_2$ are negligible as they are heavier in the spectrum. For NUHM-2 we similarly

NUHM-1	NUHM-2	NUHM-3	mSUGRA-1	mSUGRA-2
31	51	28	41	46

Table 3: *Number of events in the $SSD\tau$ channel at an integrated luminosity of 100 fb^{-1} after applying the cuts listed in Section 5.1, in addition to a cut on the R variable ($R > 0.2$) for all of our benchmark points .*

have lighter stau mass eigenstate dominated by the left-chiral component but here the mass hierarchy between the $\tilde{\tau}_1$ and the χ_1^0 is opposite to that of NUHM-1, i.e. $m_{\tilde{\tau}} < m_{\chi_1^0}$. At this benchmark point, χ_1^0 decays into $\tilde{l}\bar{l}$ pair as well as $\tilde{\nu}\nu$ pair including the third generation. The mass difference between the lighter stau and tau-sneutrino is less than m_W , hence the decay proceed mainly via the two body decay mode $\tilde{\tau}_1^\pm \rightarrow \tilde{\nu}_\tau^* \pi^\pm$ and the three body decay $\tilde{\tau}_1^\pm \rightarrow \tilde{\nu}_\tau^{(*)} l^\pm \nu^{(-)}$. However, final states with higher pion multiplicities also have non-zero branching fractions, but we have not taken into account these modes, as they do not change our conclusion. In NUHM-3, the LSP is the lightest neutralino, however we still have a light enough $\tilde{\nu}_{\tau L}$. The lighter $\tilde{\tau}_1$, of course, dominantly left-chiral here. The taus produced in SUSY cascade therefore are mostly left-chiral for all the NUHM points. The corresponding R -distributions (taking into account the SM contributions) for the respective benchmark points have been shown in Figure 2. Thus the distinction criterion set down by us is seen to survive the washouts caused by various extraneous SUSY cascades.

	NUHM-1	NUHM-2	NUHM-3	mSUGRA-1	mSUGRA-2
$\mathcal{O}_1(R < 0.8)$	0.77	0.74	0.76	0.71	0.72
$\mathcal{O}_2(R > 0.8)$	0.23	0.22	0.24	0.29	0.28
$r = \frac{\mathcal{O}_1(R < 0.8)}{\mathcal{O}_2(R < 0.8)}$	3.35	3.36	3.17	2.45	2.57

Table 4: *The ratio r for NUHM and corresponding mSUGRA scenario.*

In the corresponding mSUGRA benchmark points (mSUGRA-1 and mSUGRA-2), the lighter stau is dominantly right-chiral. However both the stau are heavier than the second lightest neutralino and lightest chargino. Taus are produced mainly via the decay of W and Z produced in the decay of $\chi_{3,4}^0 \rightarrow (\chi_1^\pm W^\mp), (\chi_2^0 h/Z), \chi_2^\pm \rightarrow (\chi_{1,2}^0 W^\pm), (\chi_1^\pm h/Z)$ and $\chi_1^\pm \rightarrow \chi_1^0 W^\pm$. Hence the contributions to $SSD\tau$ channel come from two same sign W -decay produced in SUSY cascade or one from W -decay and one in Z decay, when one of the two tau out of a Z -decay is identified. Therefore, taus are mostly left-handed, with some right-

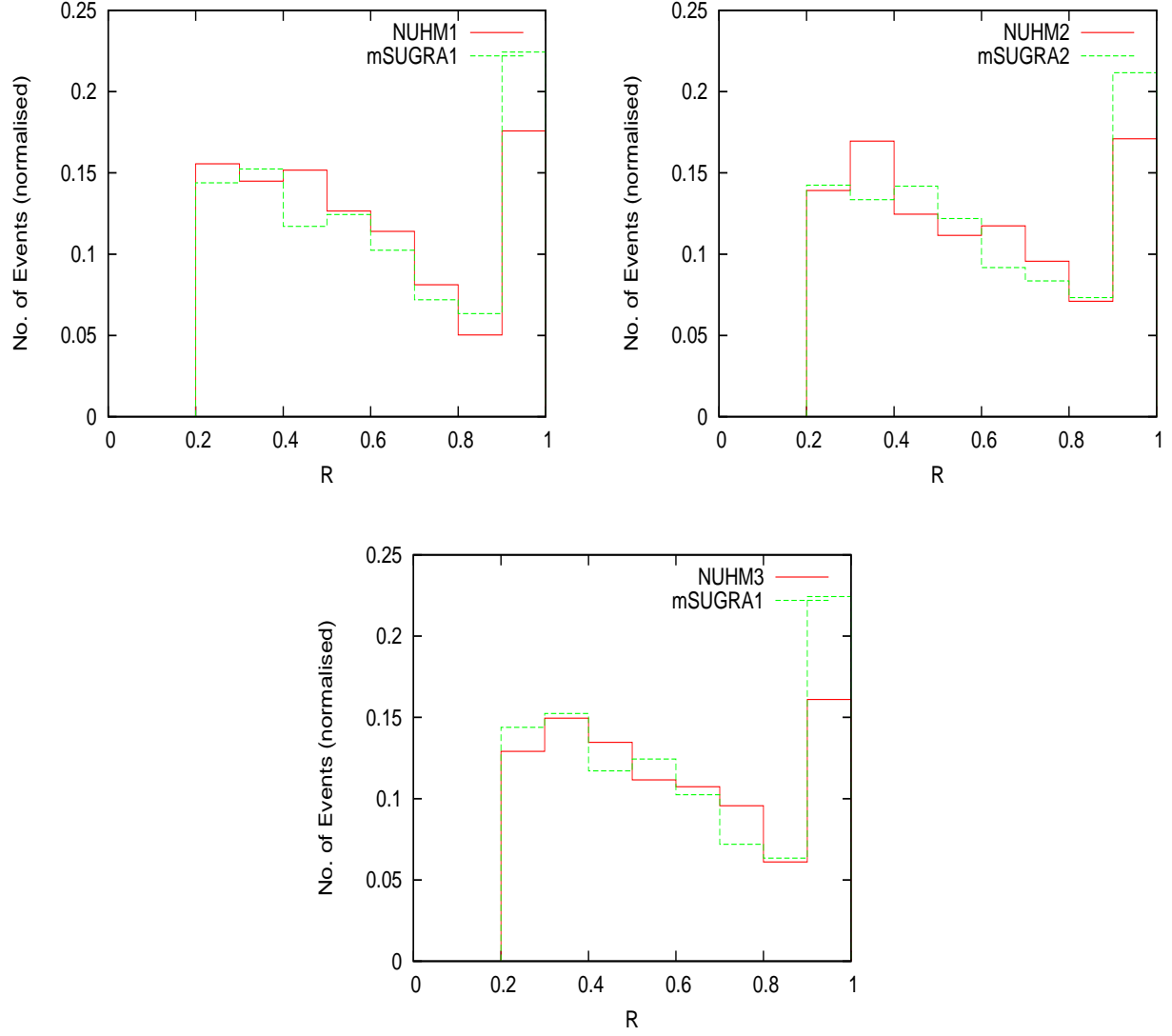


Figure 2: R distribution (defined as $R = E_{\pi^-}/E_{\tau_j}$) for NUHM scenarios and corresponding $mSUGRA$ points. A cut $R > 0.2$ has been applied in each of these distribution.

handed admixtures. This shows up in the R-distribution for the corresponding mSUGRA points with a slight departure from that of the NUHM points.

Designating the total number of events for $0.2 < R < 0.8$ and $R > 0.8$ by \mathcal{O}_1 and \mathcal{O}_2 respectively, we find that the ratio $r = \mathcal{O}_1/\mathcal{O}_2$ is a rather effective discriminator between NUHM and a corresponding mSUGRA scenario yielding a similar number of same-sign ditau events. The values of this ratio for all the cases are listed in Table 3. For the NUHM points, this ratio turn out to be consistently larger than the corresponding mSUGRA points, which is expected from the R-distribution given in Figure 2.

Lepton charge asymmetry:

The results of charge asymmetry in the jet-lepton invariant mass distribution have been shown in Figure 3 and 4. For both the NUHM-1 and NUHM-3 benchmark points, gluinos and left-chiral squarks have closely spaced masses. Therefore, the hard jets are produced either in the decay $\tilde{q}_L \rightarrow q\chi_2^0$ or in $\tilde{q}_R \rightarrow q\chi_1^0$, but not in whichever is allowed between $\tilde{g} \rightarrow q\tilde{q}_{L,R}$ or $\tilde{q}_{L,R} \rightarrow \tilde{g}q$. This is due to small mass splitting between them; even if the gluinos are lighter than the left-chiral squarks, the decay chain $\tilde{q}_L \rightarrow q\chi_2^0 \rightarrow ql_1^\pm \tilde{l}^\mp \rightarrow ql_1^\pm \tilde{l}_2^\mp \chi_1^0$ is still the dominant source of the opposite sign same flavor dilepton signal, as the decay branching ratio of $\tilde{q}_L \rightarrow q\tilde{g}$ is very small ($\simeq 2\%$ or less) due to phase-space suppression. The branching fraction for $\tilde{q}_L \rightarrow q\chi_2^0$ is $\simeq 32\%$ and subsequently χ_2^0 decays into a $\tilde{l}^\pm l^\mp$ pair with a decay branching fraction ranging from 21%-29%, while the sleptons decay into a lepton and the lightest neutralino with 100% branching ratio.

It is clear from Figure 3a and 3b that both for NUHM-1 and NUHM-3 we get the desired charge asymmetry (which is negative for increasing m_{jl} , since the lighter sleptons are dominantly left-chiral, and the leptons produced in χ_2^0 decay are mostly back-to-back with the quark while the antileptons are in the same direction to that of the quark, hence m_{jl-} distribution has larger population than m_{jl+} distribution near the end-point of m_{jl} invariant mass distribution).

The situation is somewhat more complicated for the corresponding mSUGRA points. For mSUGRA-1, the sleptons are heavier than the second lightest neutralino and the decay $\chi_2^0 \rightarrow \tilde{l}^\pm l^\mp$ is suppressed. Here the main source of the flavor subtracted opposite sign same flavor dilepton signal is the two step $\tilde{q}_L \rightarrow q\chi_2^0 \rightarrow ql^\pm \tilde{l}^\mp \chi_1^0$ decay chain rather than the three step decay chain considered earlier. In this case χ_2^0 decays into a $l^\pm \tilde{l}^\mp \chi_1^0$ pair via an off-shell slepton or Z . The sleptons are lighter than the second lightest neutralino and mostly dominated by the right-chiral component in mSUGRA-3. χ_2^0 follows its usual three step

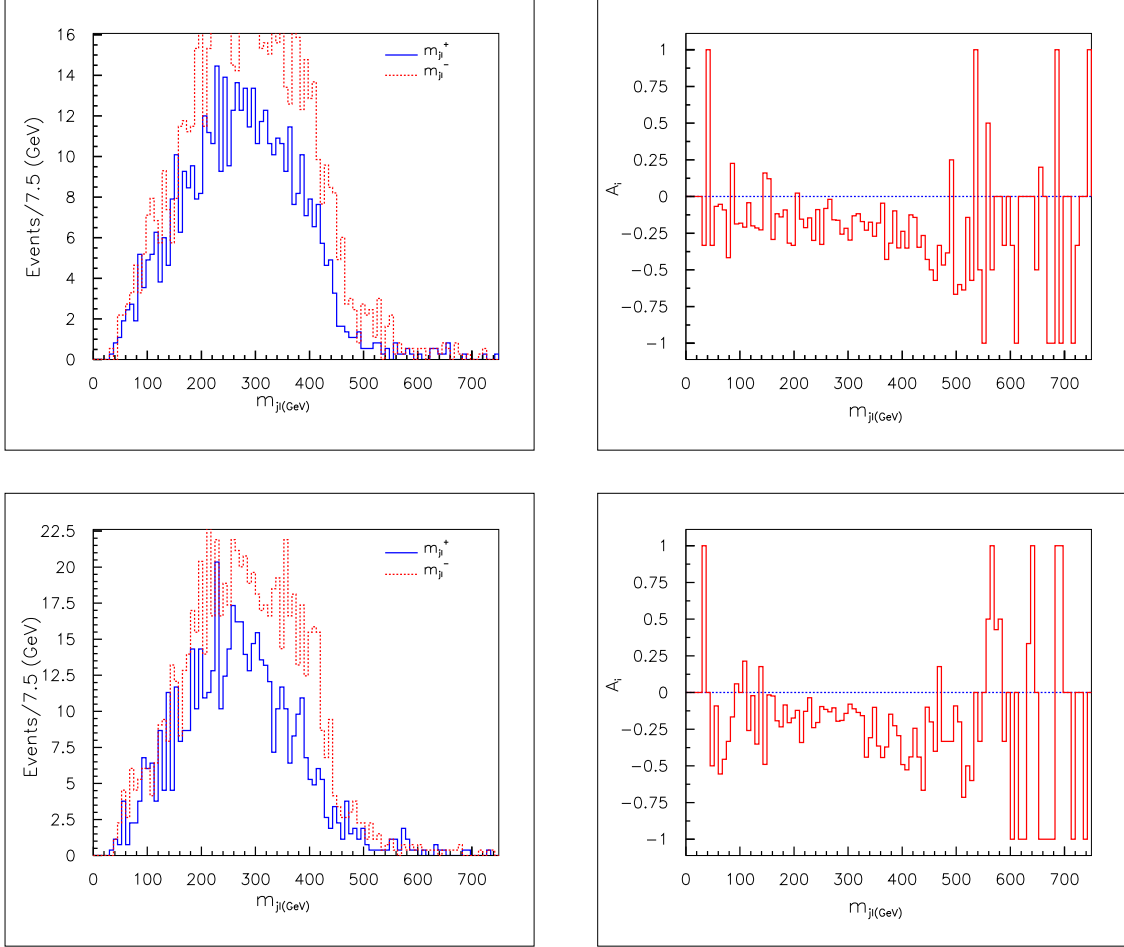


Figure 3: a) m_{jl} and b) A_i vs m_{jl} distribution for NUHM BP1 (top) and NUHM BP3 (bottom). The event rates are predicted at an integrated luminosity of 10 fb^{-1} .

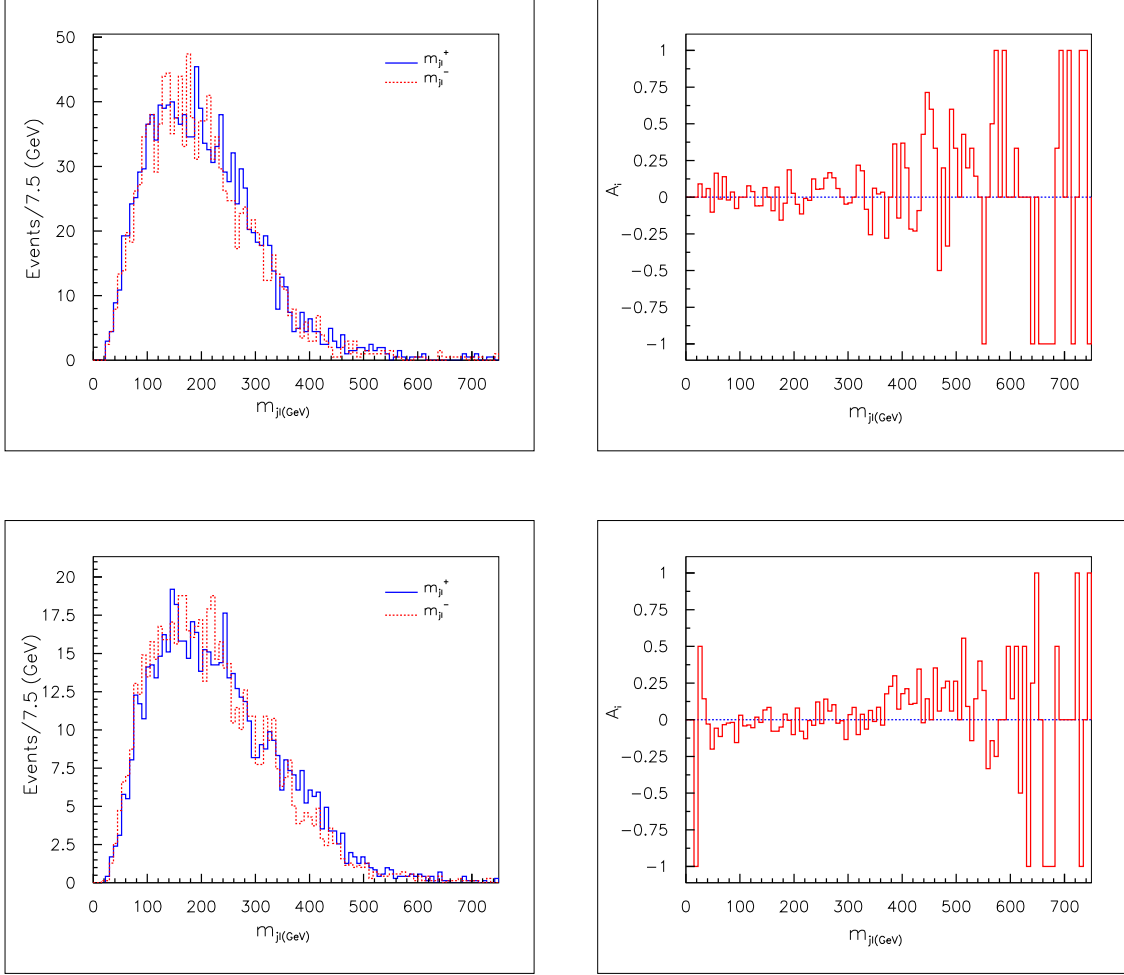


Figure 4: a) m_{jl} and b) A_i vs m_{jl} distribution for $mSUGRA$ points. The $mSUGRA-1$ (top) and $mSUGRA-3$ (bottom) corresponds to NUHM-1, and NUHM-3 benchmark points, respectively. The event rates are predicted at an integrated luminosity of 10 fb^{-1} .

decay chain. The expected positive charge asymmetry is visible for both the mSUGRA-1 and mSUGRA-3 BP's.

6 Summary and conclusion

We have attempted a differentiation between mSUGRA and a scenario with non-universal Higgs masses. The extreme situation of large negative S , for which the characteristic features of the NUHM spectrum are most prominent, has been selected for this purpose, including three possible hierarchies among the masses of the lightest neutralino, the lighter stau and the tau-sneutrino. The primary channel of investigation being tau-rich, regions in the parameter spaces of both the scenarios, giving rise to similar ditau event rates, have been pitted against each other.

In the same-sign ditau channel, we find that the ratio defined as R , the fraction of the energy carried by the charged pion in a jet produced in one-prong tau-decays, is a rather useful differentiator. Because of the dependence of R on the polarisation of the tau, one ends up having different numbers of events for the two cases in the regions $R < 0.8$ and $R > 0.8$. The ratios of these two event numbers, in turn, display a concentration in different regions, depending on whether it is NUHM or mSUGRA.

We have further suggested the utilisation of signals involving leptons of the first two families, which are largely left chiral in NUHM. A bin-by-bin analysis of the of lepton-jet invariant masses exhibits a difference between the cases with negatively and positively charged leptons, whose general nature helps one distinguishing an NUHM scenario.

If SUSY is indeed discovered at the LHC, one will certainly wish to run the machine with large integrated luminosity, so as to reveal the nature of the underlying scenario. One important question to ask in this context will be whether Higgs mass(es) have different high-scale origins compared to masses of the remaining scalars, namely, squarks and sleptons. A study in the line suggested here, based on the polarization study of tau as well as the first two family leptons, can be helpful in finding an answer to such a question.

Acknowledgment:

SB would like to thank Mihoko M. Nojiri and Theory Group, KEK and the Institute of Physics and Mathematics of the Universe for their hospitality while part of this work was being carried out. We also thank Nabanita Bhattacharya for her help during the preparation of this manuscript, and Atri Bhattacharya for computational assistance. This work was

partially supported by funding available from the Department of Atomic Energy, Government of India for the Regional Centre for Accelerator- based Particle Physics, Harish-Chandra Research Institute. Computational work for this study was partially carried out at the cluster computing facilities of KEK, Theory center and Harish-Chandra Research Institute (<http://cluster.mri.ernet.in>).

References

- [1] For reviews see for example, H. E. Haber and G. L. Kane, Phys. Rept. **117**, 75 (1985).
- [2] S. Dawson, E. Eichten and C. Quigg, Phys. Rev. D **31**, 1581 (1985); X. Tata, arXiv:hep-ph/9706307; M. E. Peskin, arXiv:0801.1928 [hep-ph].
- [3] S. P. Martin, arXiv:hep-ph/9709356, and references therein.
- [4] A. Djouadi *et al.* [MSSM Working Group], arXiv:hep-ph/9901246.
- [5] A. H. Chamseddine, R. Arnowitt and P. Nath, Phys. Rev. Lett. **49**, 970 (1982); R. Barbieri, S. Ferrara and C. A. Savoy, Phys. Lett. B **119**, 343 (1982); L. J. Hall, J. Lykken and S. Weinberg, Phys. Rev. D **27**, 2359 (1983); P. Nath, R. Arnowitt and A. H. Chamseddine, Nucl. Phys. B **227**, 121 (1983); N. Ohta, Prog. Theor. Phys. **70**, 542 (1983).
- [6] M. Dine, W. Fischler, Nucl. Phys. **B204**, 346 (1982); J. R. Ellis, L. E. Ibanez, G. G. Ross, Nucl. Phys. **B221**, 29-67 (1983); C. Kounnas, A. B. Lahanas, D. V. Nanopoulos, M. Quiros, Nucl. Phys. **B236**, 438 (1984); A. A. Anselm and A. A. Johansen, “Susy GUT With Automatic Doublet - Triplet Hierarchy,” Phys. Lett. B **200** (1988) 331; N. Polonsky and A. Pomarol, “GUT effects in the soft supersymmetry breaking terms,” Phys. Rev. Lett. **73** (1994) 2292 [arXiv:hep-ph/9406224]; R. Hempfling, “Neutrino Masses and Mixing Angles in SUSY-GUT Theories with explicit R-Parity Breaking,” Nucl. Phys. B **478** (1996) 3 [arXiv:hep-ph/9511288].
- [7] J. R. Ellis, C. Kounnas and D. V. Nanopoulos, Nucl. Phys. B **247**, 373 (1984); J. R. Ellis, K. Enqvist, D. V. Nanopoulos and K. Tamvakis, Phys. Lett. B **155**, 381 (1985); M. Drees, Phys. Lett. B **158**, 409 (1985); A. Corsetti and P. Nath, Phys. Rev. D **64**, 125010 (2001) [arXiv:hep-ph/0003186]; A. Corsetti and P. Nath, Phys. Rev. D **64**,

- 125010 (2001) [arXiv:hep-ph/0003186]; S. Bhattacharya, A. Datta and B. Mukhopadhyaya, JHEP **0710**, 080 (2007) [arXiv:0708.2427 [hep-ph]]; S. Bhattacharya, A. Datta and B. Mukhopadhyaya, Phys. Rev. D **78**, 115018 (2008) [arXiv:0809.2012 [hep-ph]].
- [8] N. Chamoun, C. -S. Huang, C. Liu, X. -H. Wu, Nucl. Phys. **B624**, 81-94 (2002) [hep-ph/0110332]; K. Huitu, J. Laamanen, Phys. Rev. **D79**, 085009 (2009) [arXiv:0901.0668 [hep-ph]]; S. P. Martin, Phys. Rev. D **79**, 095019 (2009) [arXiv:0903.3568 [hep-ph]]; S. Bhattacharya, J. Chakraborty, Phys. Rev. **D81**, 015007 (2010) [arXiv:0903.4196 [hep-ph]].
- [9] M. Drees, Phys. Lett. B **181** (1986) 279; J. S. Hagelin and S. Kelley, Nucl. Phys. B **342** (1990) 95; Y. Kawamura, H. Murayama and M. Yamaguchi, Phys. Lett. B **324** (1994) 52 [arXiv:hep-ph/9402254]; Y. Kawamura, H. Murayama and M. Yamaguchi, Phys. Rev. D **51** (1995) 1337 [arXiv:hep-ph/9406245]; A. Datta, A. Datta and M. K. Parida, Phys. Lett. B **431**, 347 (1998) [arXiv:hep-ph/9801242]; A. Datta, A. Datta, M. Drees, D. P. Roy, Phys. Rev. **D61**, 055003 (2000), [arXiv:hep-ph/9907444].
- [10] F. Gabbiani, E. Gabrielli, A. Masiero and L. Silvestrini, Nucl. Phys. B **477**, 321 (1996) [arXiv:hep-ph/9604387]; M. Misiak, S. Pokorski and J. Rosiek, Adv. Ser. Direct. High Energy Phys. **15** (1998) 795 [arXiv:hep-ph/9703442]; J. Guasch and J. Sola, Nucl. Phys. B **562** (1999) 3 [arXiv:hep-ph/9906268].
- [11] J. R. Ellis, K. A. Olive and Y. Santoso, Phys. Lett. B **539** (2002) 107, [arXiv:hep-ph/0204192]; J. R. Ellis, T. Falk, K. A. Olive and Y. Santoso, Nucl. Phys. B **652** (2003) 259, [arXiv:hep-ph/0210205].
- [12] H. Baer, A. Mustafayev, S. Profumo, A. Belyaev and X. Tata, JHEP **0507**, 065 (2005), [arXiv:hep-ph/0504001]; J. R. Ellis, K. A. Olive and Y. Santoso, JHEP **0810** (2008) 005, [arXiv:0807.3736 [hep-ph]].
- [13] A. Katz and B. Tweedie, Phys. Rev. D **81** (2010) 035012, [arXiv:0911.4132 [hep-ph]]; T. Figy, K. Rolbiecki and Y. Santoso, Phys. Rev. D **82**, 075016 (2010), [arXiv:1005.5136 [hep-ph]].
- [14] U. Chattopadhyay and D. Das, Phys. Rev. D **79**, 035007 (2009) [arXiv:0809.4065 [hep-ph]]; S. Bhattacharya, U. Chattopadhyay, D. Choudhury, D. Das and B. Mukhopadhyaya, Phys. Rev. D **81**, 075009 (2010), [arXiv:0907.3428 [hep-ph]].
- [15] M. M. Nojiri, Phys. Rev. D **51**, 6281 (1995), [arXiv:hep-ph/9412374].

- [16] R. M. Godbole, M. Guchait and D. P. Roy, Phys. Lett. B **618**, 193 (2005), [arXiv:hep-ph/0411306]; R. M. Godbole, M. Guchait and D. P. Roy, Phys. Rev. D **79**, 095015 (2009), [arXiv:0807.2390 [hep-ph]]; M. Guchait and D. P. Roy, arXiv:0808.0438 [hep-ph].
- [17] S. Y. Choi, K. Hagiwara, Y. G. Kim, K. Mawatari and P. M. Zerwas, Phys. Lett. B **648**, 207 (2007), [arXiv:hep-ph/0612237].
- [18] P. Richardson, JHEP **0111**, 029 (2001), [hep-ph/0110108].
- [19] A. J. Barr, Phys. Lett. B **596**, 205 (2004), [arXiv:hep-ph/0405052].
- [20] T. Goto, K. Kawagoe, M. M. Nojiri, Phys. Rev. **D70**, 075016 (2004), [hep-ph/0406317]; S. K. Mandal, M. Nojiri, M. Sudano and T. T. Yanagida, JHEP **1101**, 131 (2011), [arXiv:1004.4164 [hep-ph]].
- [21] A. Djouadi, J. L. Kneur and G. Moultaka, Comput. Phys. Commun. **176**, 426 (2007), [arXiv:hep-ph/0211331].
- [22] C. Amsler *et al.* [Particle Data Group], Phys. Lett. B **667**, 1 (2008).
- [23] A. Djouadi, M. Drees and J. L. Kneur, JHEP **0603**, 033 (2006), [arXiv:hep-ph/0602001].
- [24] E. Komatsu *et al.* [WMAP Collaboration], Astrophys. J. Suppl. **192**, 18 (2011), [arXiv:1001.4538 [astro-ph.CO]].
- [25] J. R. Ellis, K. A. Olive, Y. Santoso and V. C. Spanos, Phys. Lett. B **588**, 7 (2004), [arXiv:hep-ph/0312262]; J. L. Feng, S. Su and F. Takayama, Phys. Rev. D **70**, 075019 (2004), [arXiv:hep-ph/0404231].
- [26] K. Hagiwara, A. D. Martin and D. Zeppenfeld, Phys. Lett. B **235**, 198 (1990); B. K. Bullock, K. Hagiwara and A. D. Martin, Phys. Rev. Lett. **67**, 3055 (1991).
- [27] S. Raychaudhuri and D. P. Roy, Phys. Rev. D **52**, 1556 (1995), [arXiv:hep-ph/9503251].
- [28] H. L. Lai *et al.* [CTEQ Collaboration], Eur. Phys. J. C **12**, 375 (2000), [arXiv:hep-ph/9903282].

- [29] S. Jadach, J. H. Kuhn, Z. Was, Comput. Phys. Commun. **64**, 275-299 (1990); Z. Was, P. Golonka, Nucl. Phys. Proc. Suppl. **144**, 88-94 (2005), [hep-ph/0411377]; P. Golonka, B. Kersevan, T. Pierzchala, E. Richter-Was, Z. Was, M. Worek, Comput. Phys. Commun. **174**, 818-835 (2006), [hep-ph/0312240].
- [30] T. Sjostrand, S. Mrenna and P. Skands, JHEP **0605**, 026 (2006), [arXiv:hep-ph/0603175].
- [31] M. Muhlleitner, A. Djouadi and Y. Mambrini, Comput. Phys. Commun. **168**, 46 (2005) [arXiv:hep-ph/0311167].
- [32] S. Biswas and B. Mukhopadhyaya, Phys. Rev. D **79**, 115009 (2009), [arXiv:0902.4349 [hep-ph]].
- [33] G. Marchesini, B. R. Webber, G. Abbiendi, I. G. Knowles, M. H. Seymour and L. Stanco, Comput. Phys. Commun. **67**, 465 (1992); G. Corcella *et al.*, JHEP **0101**, 010 (2001), [arXiv:hep-ph/0011363]; S. Moretti, K. Odagiri, P. Richardson, M. H. Seymour and B. R. Webber, JHEP **0204**, 028 (2002), [arXiv:hep-ph/0204123].
- [34] F. E. Paige, S. D. Protopopescu, H. Baer and X. Tata, arXiv:hep-ph/0312045.
- [35] E. Richter-Was, arXiv:hep-ph/0207355.
- [36] The CMS Collaboration, CMS-TDR-8.1, CERN/LHCC 2006-001.
- [37] G. Aad *et al.* [The ATLAS Collaboration], [arXiv:0901.0512].